Mechanism by which the Prone Position Improves Oxygenation in Acute Lung Injury

WAYNE J. E. LAMM, MICHAEL M. GRAHAM, and RICHARD K. ALBERT

Departments of Medicine and Radiology, University of Washington, Seattle, Washington

The mechanism by which oxygenation improves when patients with ARDS are turned from supine to prone position is not known. From results of our previous studies we reasoned that (*1*) when supine, in the setting of lung injury, transpulmonary pressure will be less than airway opening pressure and (2) atelectasis will develop preferentially in dorsal lung areas, and (*3*) both ventilation and ventilation/perfusion ratios would improve in these regions on turning prone. To study this directly, we measured regional ventilation and perfusion using ^{81m}Kr and ^{99m}Tc-MAA, respectively, and single photon emission computed tomography, both prone and supine, in four control animals and four given oleic acid. After oleic acid, the prone position improved (*1*) oxygenation (mean ± SD Pa_{O_2} = 140 ± 112 versus 453 ± 54 mm Hg), (2) median ventilation/perfusion ratios (0.77 versus 0.95), (*3*) ventilation/perfusion heterogeneity (coefficient of variation 86 ± 15 versus 61 ± 6), and (*4*) the gravitational ventilation/perfusion gradient (dependent to non-dependent slopes of 0.22 versus −0.02, all $p < 0.05$). The prone position generates a transpulmonary pressure sufficient to exceed airway opening pressure in dorsal lung regions, i.e., in regions where atelectasis, shunt, and ventilation/perfusion heterogeneity are most severe; without adversely affecting ventral lung regions.
Lamm WJE, Graham MM, and Albert RK. Mechanism by which the prone position improves oxygenation in acute lung injury. Am J Respir Crit Care Med 1994;150:184-93.

In 1977, Douglas and colleagues (1) reported that oxygenation improved in six of six patients with ARDS who were turned from supine to prone position. Two other studies have confirmed this observation in an additional 17 adult patients (2, 3). Of the 23 patients studied, oxygenation improved in 16 (70%) to such an extent that the level of positive end-expiratory pressure and/or the fraction of inhaled oxygen could be reduced.

The mechanism by which the prone position has this beneficial effect has not yet been elucidated. Proposed explanations include a prone position-induced (*1*) increase in functional residual capacity (FRC), (2) change in regional diaphragm motion, (*3*) redistribution of perfusion (Q) along a gravitational gradient toward less injured lung regions, and (*4*) better secretion removal (1–3).

To investigate these mechanisms, we have utilized an animal model of acute lung injury and noted that (a) oxygenation improves markedly on turning from supine to prone position (mean increase approximately 100 mm Hg on 100% O_2), (b) the improvement occurs within minutes of the turn, lasts for at least 30 min, reverses within 5 min on turning back to the supine position, and rapidly returns on returning to the prone position, (c) does not diminish over at least 3 h, and (d) results primarily from reduction in shunt, without change in FRC or regional diaphragm movement, and without gravitational redistribution of perfusion to less injured areas of lung (4–6).

Because we noted that shunt decreased in the prone position while the regional distribution of perfusion (Qr) changed very little, we inferred that the primary effect of turning prone must be to improve regional ventilation (Vr) and sought evidence explaining how this might occur. Several investigators have recently demonstrated that the gravitational distribution of pleural pressure (Ppl) is much more uniform (i.e., there is less gravitational gradient) when animals are prone compared with when they are supine (7–9). Accordingly, we measured Ppl in the dependent and non-dependent lung regions of supine and prone animals, before and after creating pulmonary edema with volume overload (10). We confirmed that the gravitational Ppl gradient was less when the animals were prone (both before and after volume infusion). We also found that, after creating edema, Ppl in the dependent lung region became *positive* when the animals were supine, and was much less positive when they were turned prone. This finding suggested that when animals are supine, dorsal lung regions might be below closing volume (i.e., that the transpulmonary pressure (Ptp) at end-inhalation in this region might not exceed airway opening pressure). The less positive Ppl in dependent (i.e., ventral) regions that results from turning prone, along with the more uniform Ppl gradient that exists in this position, could cause much less of the lung to be below closing volume. If these hypotheses were correct, ventilation would be diminished or absent relative to perfusion in the dorsal lung regions when animals were supine, but would increase on turning prone without decreasing V/Q ratios in ventral regions. Accordingly, we designed the following study to visualize the relative Vr/Qr in acutely injured lungs to determine which areas are affected by turning from supine to prone.

(Received in original form July 15, 1993 and in revised form December 8, 1993)

Correspondence and requests for reprints should be addressed to Richard K. Albert, M.D., Pulmonary and Critical Care Medicine, RM-12, University of Washington Medical Center, Seattle, WA 98195.

METHODS

Animal Preparation

Eight adult mongrel dogs (four female, four male, 17.5 ± 2.2 [SD] kg) were studied. Protocols and procedures were approved by the University of Washington Animal Care Committee. Anesthesia was induced with intravenous thiamylal sodium (18 mg/kg) followed by pentobarbital sodium (11 to 15 mg/kg) and was maintained with pentobarbital sodium (30 mg), ketamine hydrochloride (33 mg), and diazepam (0.8 mg) every half hour or as needed. The dogs were put in the supine position on a heating pad, intubated, and mechanically ventilated with room air using a tidal volume of 12 ± 1 (SD) ml/kg and a rate of 26 ± 2 breaths/min. A catheter was placed in the carotid artery to measure systemic arterial pressure (Psa) and to obtain blood for arterial blood gas (ABG) analysis (reported as the alveolar-arterial O_2 difference [A-aDO_2] assuming that the respiratory quotient [RQ] = 0.8). A Swan-Ganz catheter was inserted in the jugular vein to monitor pulmonary arterial pressure (Ppa) and to measure cardiac output (CO), as well as to inject radiolabeled markers. Mean Psa, Ppa, and peak airway pressure (P_A) were directly calculated and recorded by computer. Vascular pressures were referenced to the mid-chest.

Four dogs were used as controls and four received oleic acid (OA) to produce acute lung injury. Those receiving OA were placed on 100% oxygen prior to injection of 0.09 ml/kg OA (Sigma Chemical Co., St. Louis, MO) over 8 min through a 25-gauge needle into a normal saline drip that was being continuously infused via the proximal port of the Swan-Ganz catheter. During OA infusion the dogs were rotated through 360° in four positions (supine, left lateral decubitus, prone, right lateral decubitus) in an attempt to produce a uniform injury as we have demonstrated occurs with this maneuver (5). The injury was allowed to develop for 75 to 120 min, during which time the saline drip was continued (total vol received = 400 to 500 ml) and sodium bicarbonate was given as needed to maintain the arterial blood pH > 7.30 prior to beginning data collection. All animals were subsequently treated in an identical fashion.

Protocol

Half of the control and half of the OA-injured animals were initially studied in the supine position and the other half were initially studied prone to nullify any potential effect of sequence or time-dependent effects on the results. Each animal received a sigh breath consisting of three times their tidal volume, after which CO was measured followed by ABGs and body temperature. For the initial determination of Qr, ventilation was temporarily stopped at end-exhalation and ^{99m}Tc-MAA (1.5 mCi) was injected into the proximal port of the Swan-Ganz catheter over approximately 15 s. This dose produced an external count rate of ~ 3,000 to 4,000/s when the whole lung was imaged by single-photon emission-computed tomography (SPECT). The SPECT system included a GE 400 AT rotating gamma camera (General Electric Medical Systems, Milwaukee, WI) and an ADAC 3300 computer (ADAC Laboratories, Sunnyvale, CA). Images were acquired in a 64 × 64 matrix, 30 s/image, with 64 images over 360° rotation.

Immediately following this initial determination of Qr, and without moving the animal, Vr was measured by obtaining another SPECT scan while ventilating the lungs with ^{81m}Kr (Krypton Gas Generator; MPI Pharmacy Services Inc., Seattle, WA). ^{81m}Kr was delivered to the lungs by blowing warm, humidified gas through the generator and into the intake line of a ventilator (Model 607; Harvard Apparatus, Millis, MA) that was modified to deliver gas directly from the piston into the endotracheal tube, bypassing the normal inspiratory valve and tubing to reduce the dead space between the generator and the animal and thereby maximize the amount of active ^{81m}Kr (half life = 13 s) entering the lungs. The Vr scans also consisted of 64 frames, each acquired over 30 s at a count rate of ~1,100 to 1,400/s.

When the first Vr scan was completed, the animal was then rotated to the opposite position (prone or supine) and allowed to stabilize for ~ 10 min, after which a second Vr scan was performed. Then a second Qr scan was obtained to determine the residual or background counts that were present as a result of the initial ^{99m}Tc-MAA injection. A second injection of ^{99m}Tc-MAA was then given at end-exhalation at a larger dose (15 mCi) producing a count rate of ~ 20,000 to 40,000/s, and a third Qr scan was then obtained, consisting of 64 frames of 10 s duration.

At the end of the experiment, the animal was killed with T-61 solution (Hoechst-Roussel Agri-Vet Co., Decatur, IL).

Tomographic Reconstruction

Data from the 64 images obtained during rotation of the gamma camera were reconstructed using a binomial three point (0.25, 0.50, 0.25) filter in the Z axis, a 0.7 pixel^{-1} Butterworth order 5 filter for the ^{99m}Tc (perfusion) studies, and a 0.9 pixel^{-1} Butterworth order 5 filter for the ^{81m}Kr (ventilation) studies for both X and Y axes. These filters produced similar full-width half-maximum (FWHM) values of 2 cm for both the Vr and Qr scans, although each voxel represented a lung area of ~ 0.67 × 0.67 × 0.67 cm^3. No attenuation corrections were used in comparing ratios of Vr with Qr since there is very little difference in attenuation between 140 KeV (^{99m}Tc) and 190 KeV (^{81m}Kr). Reconstructed images were transferred to a Macintosh IIci computer for further manipulation and analysis.

Preliminary Data Manipulation

In each position the Vr and Qr images were combined into one data set. Since the dog was not moved between the scans done in any single position, the X, Y, Z coordinate system corresponded to the same volume of lung in each image.

To reduce the data set of 262,144 voxels to those that contained only lung, we considered that all voxels with Q counts < 150 after the initial injection of ^{99m}Tc-MAA and < 250 after the second injection consisted of background and discarded them. Mean ± SD counts/pixel in the lung were 1,340 ± 992 supine and 1,325 ± 661 prone. Using a three-dimensional graphics program (JMP Version 2; SAS Institute Inc., Cary, NC), the images were rotated and subjectively additional voxels that were separate from the lung image were deleted. The result was an image set consisting of corresponding Vr/Qr mapped in X, Y, and Z coordinates. Images obtained in the second position (supine or prone) were corrected for background radioactivity resulting from the initial ^{99m}Tc-MAA injection by subtracting the counts recorded in the second Qr scan from those measured in the third.

Relative Vr/Qr was calculated by dividing Vr to each voxel by Qr to each voxel and then dividing by the mean Vr/Qr to obtain a relative Vr/Qr for all voxels.

Microsphere Studies

The ability of SPECT to represent Qr was tested in three of the control animals by comparing Qr measured by SPECT with that measured by radiolabeled microspheres. At the time of each injection of ^{99m}Tc-MAA, one of five radioactive 15-μm diameter microspheres (^{141}Ce, ^{113}Sn, ^{103}Ru, ^{95}Nb, or ^{46}Sc; Dupont, NEN Research Products, Boston, MA) was also injected into the proximal port of the Swan-Ganz catheter. Adequate numbers of microspheres were injected to insure that > 2,500 would be present in each piece of lung (6). At the end of these experiments, the animals were heparinized and exsanguinated before being killed. The intact lungs were inflated to 40 cm H_2O (~ TLC) and another SPECT perfusion scan was obtained. A radio-opaque marker was placed on the lungs and a lateral chest X-ray was taken to assist in subsequent alignment in the true isogravitational plane. The lungs were then removed, air dried, and diced, and the radioactivity in each piece was determined as previously described (6). In brief, the lungs were flushed clear of blood with saline, removed from the chest, and air dried at 25 cm H_2O, after which they were placed vertically in a box and embedded in urethane foam (2 lb Polyol and Isocyanate; International Sales, Seattle, WA). A miter box was used to cut the foam block into uniformly sized cubes that were ~ 1.95 cm^3 in volume. Adhering foam was removed from the lung tissue, each piece was assigned its three-dimensional coordinate and weighed, and radioactivity was determined in a 3 × 3.25-in sodium well crystal gamma counter (Minaxi gamma counting system, model 5550; Packard, Downers Grove, IL). Each sample was corrected for decay time and spillover by the matrix inversion method (6). Pieces weighing < 10 mg or > 60 mg were discarded due to the relative error in weighing the smaller pieces, and the likelihood that the larger pieces contained non gas-exchanging tissue which would make weight normalization inappropriate. The relative flow to each lung piece was calculated by dividing the measured radioactivity of each piece

by the mean radioactivity of all pieces. Relative flow was divided by the weight of each piece and normalized to the mean piece weight, providing a weight-normalized relative flow per piece. The three-dimensional array of normalized flow was then reconstructed and analyzed on a computer and compared with the data calculated by the perfusion SPECT scans at TLC.

Estimation of Vr/Qr Corresponding to Shunt

The resolution of SPECT scanning is such that two points must be ~ 2 cm apart before they can be distinguished as separate. This means a sphere of perfused lung approximately 33.5 cm^3 ($V = 4/3\ \pi r^3$) would have to receive no V to produce a single voxel with a Vr/Qr of 5% of the surrounding value. Areas of shunt smaller than 33.5 cm^3 adjacent to regions of low or normal V/Q would have a relative Vr/Qr measured by SPECT that represented a weighted average Vr/Qr present in entire 33.5 cm^3 region, and would therefore underestimate the degree of abnormality. Accordingly, to estimate the relative Vr/Qr equating to shunt, we determined the percent shunt in the prone position after OA using the A-aDO_2 measured on 100% O_2 (assuming an arterial-venous O_2 content difference of 5 ml/100 ml blood). We then determined the relative Vr/Qr ratio that would identify the same percent of voxels. This ratio, once obtained for a specific animal, was applied to that animal's data recorded in the other conditions.

Statistical Analysis

Values are presented as mean ± SD in the tables and ± SEM in the figures. Hemodynamic and gas exchange variables were measured before obtaining both the Vr and the Qr scans in each animal in both positions. The data presented represent the mean of the two values. The gravitational gradient of relative Vr/Qr was determined by the standard two-stage method (11). Medians, skew, and coefficients of variation were used to characterize the distribution of Vr/Qr throughout the lungs in supine and prone positions and were compared using Student's paired *t* test. Comparisons between control and OA-treated animals were performed using Student's unpaired *t* test. $p < 0.05$ was considered significant.

RESULTS

Hemodynamics and Gas Exchange

As shown in Table 1, for control animals pulmonary vascular pressures, CO and ABGs were similar in supine and prone positions (all $p > 0.05$). In the animals receiving OA, CO fell relative to pre-OA values and was also lower than that of the control animals regardless of position (all $p < 0.05$) but no supine-to-prone differences in pressures or CO were observed. As we have previously observed, the A-aDO_2 was greatly improved in the prone position ($p < 0.01$). During the 30 min required for SPECT scanning after OA, the A-aDO_2 decreased 7% in the supine position (p = NS) and 28% in the prone position ($p < 0.05$).

Accuracy of SPECT Scanning

To evaluate the accuracy of our method for detecting the edge of the lung on SPECT images (i.e., distinguishing the point at which counts represented Q in lung, as opposed to background noise) we compared the dimensions of control lungs scanned by SPECT at TLC with the actual dimensions of each lung measured after removal and air-drying at TLC. The maximum length in each of the three coordinates (X, Y, and Z) for the SPECT scans averaged (± SD) 16.9 ± 0.8, 14.1 ± 0.4, and 24.4 ± 0.7 cm, respectively. Measurements obtained directly from slices of the air-dried lung were 16.7 ± 0.3, 16.3 ± 0.3, and 24.7 ± 0.6 cm (X, Y, Z; respectively, $p < 0.05$ in the Y axis only).

Inherent resolution limitations of SPECT require that data be filtered during the reconstruction process. We chose high-resolution filters that provided as little smoothing as possible but still limited the amount of noise. We limited our analysis to *relative* Vr/Qr which will accurately reflect true Vr/Qr if the FWHM for both the Q and V scans are the same. To test the validity of this assumption, we imaged a narrow i.v. tube surrounded by 1 L bags of normal saline, through which ^{81m}Kr was passed. Then, without moving the tube, we re-imaged it after it was filled with ^{99m}Tc-MAA. If the choice of filters were appropriate, the absolute counts of the two isotopes would have a relatively constant ratio throughout any region of interest despite marked voxel-to-voxel variations in both. A constant ratio was observed with sharp edge detection with 0.9 and 0.7 $pixel^{-1}$ Butterworth filters selected for V and Q, respectively (Figure 1).

A representative comparison of relative Qr measured at TLC by post-mortem SPECT scanning with that measured by radiolabeled microspheres is shown in Figure 2. Both methods demonstrated that flow diminished in the periphery (both ventral and dorsal edges). By SPECT scanning (of two animals studied prone and one supine) the median Qr, skew, and coefficient of variation were 0.90 ± 0.1, 0.46 ± 0.3, and 48.7 ± 13.3 (mean ± SD), respectively. By microspheres the values were 1.00 ± 0.15 ($p = 0.07$), −0.4 ± 0.3 ($p < 0.01$), and 32.1 ± 1.1 ($p > 0.1$), respectively. Thus, relative to the data observed using microspheres, the median relative Qr measured by SPECT was shifted to a value slightly below 1, skewed toward Qr values > 1, and was somewhat more variable.

The above comparison was done at TLC. Because we measured relative Vr/Qr during tidal breathing (i.e., between FRC and FRC + tidal volume), we also addressed the effect of stopping ventilation and inflating the lung to TLC on the distribution of microspheres injected during ventilation. The general pattern of Qr was again similar under the two conditions, but inflating to TLC

TABLE 1

HEMODYNAMIC AND RESPIRATORY VALUES FOR FOUR CONTROL AND FOUR OA INJURED, VENTILATED ANIMALS

	Psa (*mean*)	Ppa (*mean*)	PA (*max*)	CO (*L/min*)	pH	Pco_2 (*mm Hg*)	Po_2 (*mm Hg*)	$AaDo_2$ (*mm Hg*)	% Shunt
Control									
Supine	130 ± 11	13 ± 7	9 ± 2	2.5 ± 0.2	7.37 ± 0.05	42 ± 4	99 ± 5	2 ± 3	–
Prone	145 ± 23	17 ± 8	9 ± 3	3.3 ± 0.5	7.35 ± 0.02	42 ± 3	105 ± 5	−5 ± 7	–
Oleic Acid									
pre-OA supine	135 ± 10	14 ± 1	9 ± 2	3.3 ± 0.6	7.41 ± 0.06	33 ± 5	567 ± 21§	113 ± 25§	5.6 ± 1.2§
Supine	121 ± 29	17 ± 4	12 ± 2	1.9 ± 0.4†‡	7.35 ± 0.05†	40 ± 6	140 ± 112†	533 ± 109†‡	22.1 ± 8.2†
Prone	129 ± 29	15 ± 4	10 ± 2	2.0 ± 0.1‡	7.36 ± 0.05	41 ± 4	453 ± 54*‡	219 ± 51*‡	10.5 ± 3.1*

Values are expressed as mean ± SD. Control = air and OA = 100% O_2.

Methods for determining % shunt are explained in the text and were not possible for the control group.

* Supine versus prone positions within groups and †, pre- versus post-OA supine ($p < 0.05$, Student's paired *t* test).

‡ Control versus OA in the same body position ($p < 0.05$, Student's unpaired *t* test).

§ Only three of the four animals for the pre-OA data as one animal was inadvertently ventilated with < 100% O_2 due to a leak in the ventilation tubing.

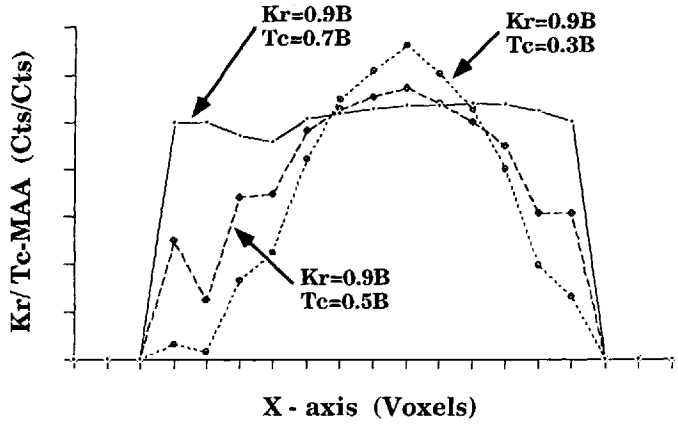

Figure 1. Ratio of $^{81m}Kr/^{99m}Tc$-MAA in a region of interest drawn through reconstructed images of an i.v. tube surrounded by 1 L bags of normal saline as a function of various frequency cutoff filters. B = Butterworth filter (frequency cutoff). The combination of filters selected (Butterworth 0.9 and 0.7 pixel^{-1} for V and Q scans, respectively) gives uniform V/Q ratios despite wide variations in V and Q, and sharply delineates the edge.

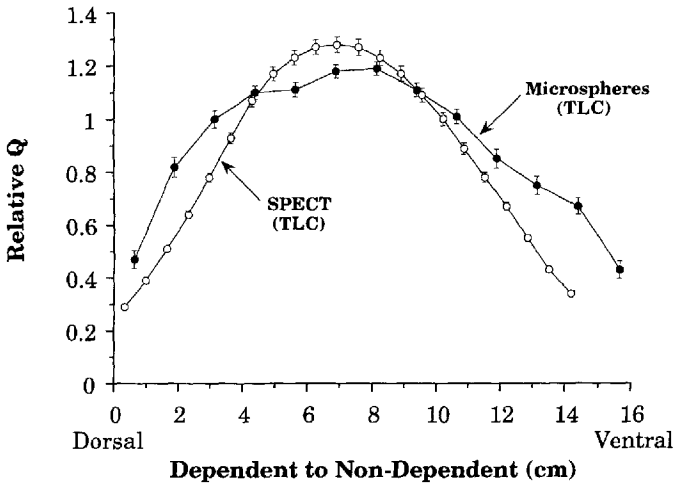

Figure 2. Mean (± SEM) Vr/Qr for each isogravimetric coronal slice of a representative supine dog determined by SPECT scans (^{99m}Tc-MAA) and by radiolabeled microspheres. Isotopes injected at FRC and analyzed at TLC.

shifted the median relative Qr to the right compared with that seen during tidal breathing (0.81 ± 0.04 versus 0.91 ± 0.07, $p < 0.05$); no effect on skew or the coefficient of variation was observed (0.88 ± 0.06 versus 0.46 ± 0.26 and 63.6 ± 7.3 versus 48.7 ± 13.3, both $p > 0.1$). These observations were expected, as inflating to TLC would expand dependent lung regions more than nondependent ones and this would distribute microspheres in the dependent region more uniformly. Liu and colleagues (8) and Reed and Wood (10) have previously noted that the maximal displacement of microspheres due to parenchymal expansion from FRC to TLC is only 1 to 2 cm.

The studies comparing perfusion measured by microspheres with that measured by SPECT were always done following injection of 15 mCi of ^{99m}Tc-MAA. When less ^{99m}Tc-MAA was used (1.5 mCi) each of the 64 scanning frames was collected over 30 s (as opposed to the 10-s interval used with the higher dose of radioactivity) to reduce potential problems caused by the larger noise-to-signal ratio.

Relative Distribution of Vr/Qr (Supine versus Prone)

Figures 3 (control) and 4 (OA) show the frequency distributions of relative Vr/Qr for all eight animals, measured supine and prone. Since CO decreased after OA but minute ventilation was unchanged, the absolute Vr/Qr was higher in those animals receiving OA than it was in the control animals.

In control animals the median Vr/Qr shifted toward 1 and the mean coefficient of variation was reduced on turning prone (Figure 3, Table 2, both $p < 0.05$). In the supine position a small but significant direct relationship between relative Vr/Qr and height up the gravitational plane was present (Table 2). No such relationship was observed when animals were prone.

OA-induced injury increased the coefficient of variation and the gravitational distribution of relative Vr/Qr (Figures 3 and 4, Table 2, both $p < 0.05$). The median relative Vr/Qr and the coefficient of variation were improved by turning prone (both $p < 0.05$) and again, no gravitational relative Vr/Qr relationship was apparent (Figure 4, Table 2).

Spatial Relationship of Relative Vr/Qr (Supine versus Prone)

The relative Vr/Qr in four transverse slices of each control lung is shown in Figure 5, and in four lungs injured with OA in Figure 6.

In control animals, an area of rather low Vr/Qr was apparent in the dorsal regions of both lungs when animals were supine, and the relative Vr/Qr in this area improved when they were turned prone.

After OA, all four lungs showed large areas in the dorsal regions in which relative Vr/Qr was < 0.3 (i.e., ~ equivalent to shunt) when animals were supine, and relative Vr/Qr in this area markedly improved when they were turned prone. Small areas with high relative Vr/Qr were also apparent in the ventral regions when animals were supine. Although relative Vr/Qr in these regions decreased when animals were turned prone, the volume of lung in which the relative Vr/Qr improved far exceeded that in which it worsened (Figure 6, Table 2).

DISCUSSION

The important findings of this study are that in the canine OA-induced model of acute lung injury, turning from supine to prone (*1*) increases oxygenation, (2) shifts median relative Vr/Qr toward more normal values, (*3*) decreases relative Vr/Qr heterogeneity, and (*4*) causes these improvements to occur primarily in dorsal lung regions.

We elected to eliminate voxels containing background activity by thresholding on Q rather than on V scans, reasoning that Q in the lung was less likely to approach zero in any given voxel than was V after OA injury. The threshold selection omitted no voxels located in the main portion of the lung images but may have eliminated some that were located on the outer edges. The close approximation between lung dimensions estimated from SPECT scans and those obtained directly from excised lungs suggests this method was acceptable. Similarly, the relatively constant ratio of ^{81m}Kr to ^{99m}Tc-MAA indicates that our choice of filters was appropriate and that edge effects for relative Vr and Qr would be similar.

By expressing Vr relative to Qr, differences in chest wall attenuation for the two isotopes were nullified and the denominators of Vr and Qr (e.g., units of gas volume or lung tissue) were canceled out. Expressing Vr as a function of mean V, and Qr as a function of the mean Q generates relative Vr/Qr ratios, rather than absolute values.

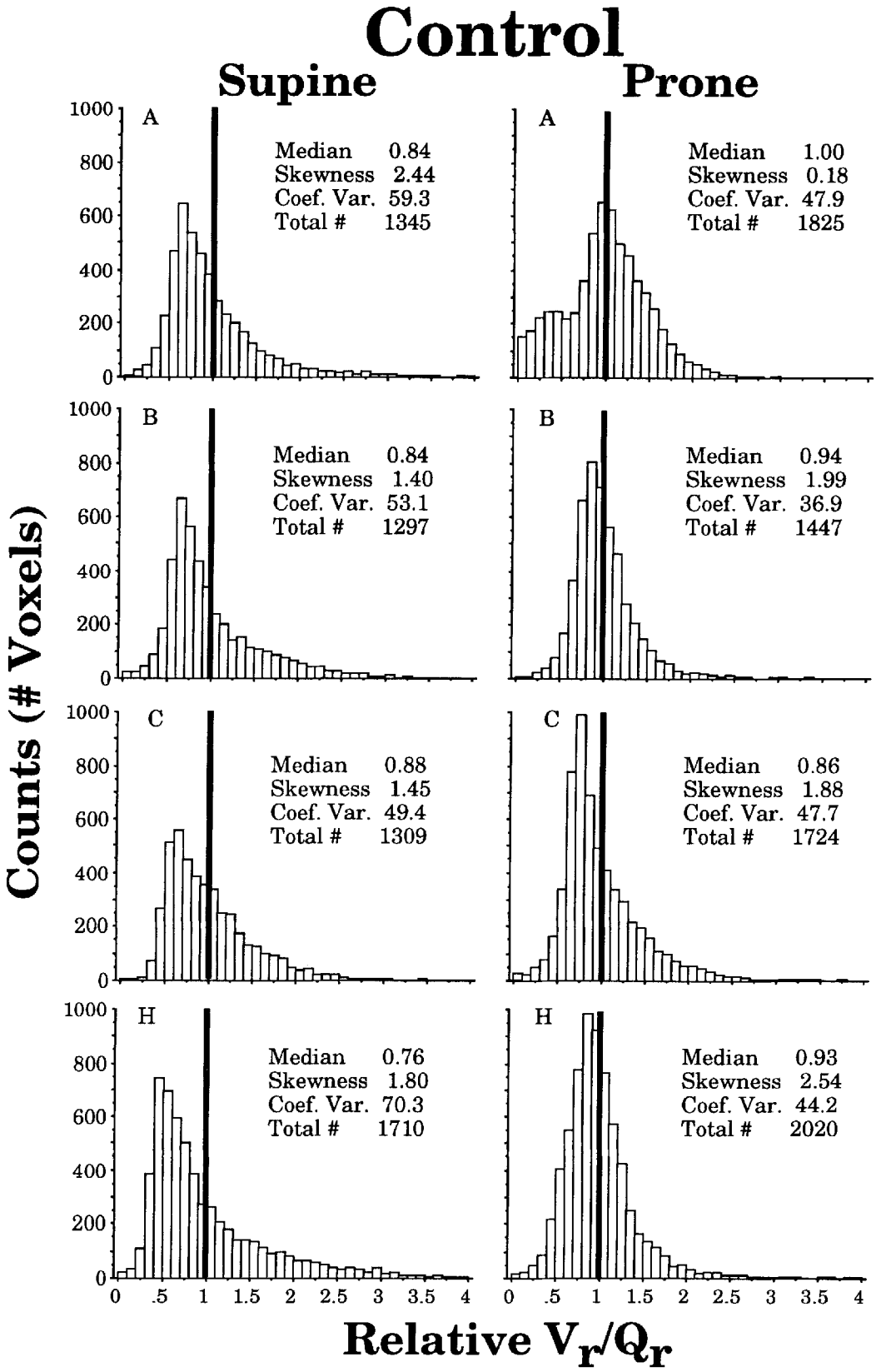

Figure 3. Frequency distribution of relative Vr/Qr for each control animal in the supine and prone condition. Capital letters represent individual animals.

TABLE 2

DISTRIBUTION OF VENTILATION TO PERFUSION RATIO IN FOUR CONTROL AND FOUR OA INJURED, MECHANICALLY VENTILATED DOGS

	Relative V/Q				
	Distribution			Linear Regression	
	Median	Skew	Coefficient of Variation	versus Y (slope)‡ Dep-NonDep	r2
Control					
Supine	0.83 ± 0.05	1.8 ± 0.5	58 ± 9	0.12 ± 0.30§	0.38 ± 0.14
Prone	0.94 ± 0.06*	1.6 ± 1.0	44 ± 5*	0.00 ± 0.05*	0.10 ± 0.08
Oleic Acid					
Supine	0.77 ± 0.15	1.4 ± 0.6	91 ± 16†	0.22 ± 0.04†§	0.53 ± 0.10
Prone	0.95 ± 0.08*	1.5 ± 0.5	61 ± 5*†	−0.02 ± 0.09*	0.15 ± 0.12

Values are expressed as mean ± SD.

* $p < 0.05$, supine versus prone within groups (Student's one-tailed paired *t* test).

† $p < 0.05$, control versus OA in the same body position (Student's two-tailed unpaired *t* test).

‡ Change in relative V/Q/cm.

§ $p < 0.05$, slope different than zero (Student's two-tailed unpaired t test).

We measured a 10.5% shunt in prone animals breathing 100% O_2 after OA, subsequently determined that a relative Vr/Qr < 0.3 described 10.5% of the voxels measured by SPECT, and then utilized this lower limit of Vr/Qr to represent shunt in the other conditions. Although the quantity of shunt we report in the supine and prone positions would be altered if a different relative Vr/Qr were used to make this estimate, the qualitative effects of the position change would not, as choosing a different relative Vr/Qr would have no effect on the regional distribution of lung regions having a Vr/Qr less than the selected value. It is of interest to note, however, that the shunts we estimated in the present study were very similar to those we measured previously using the multiple inert gas elimination technique (MIGET) (1). In this earlier report, intrapulmonary shunt ranged from 7 to 18% in the prone position (after OA) and increased to 20 to 34% when animals were turned supine. Despite the fact that the resolution of SPECT does not allow separation of ventilated from non-ventilated regions at the alveolar level, the degree of shunt estimated in the present study (Table 1) correlated well with what we previously measured directly, and the effect of position on shunt was also similar.

Although we did not assess the uniformity of injury in the present study, we did so in considerable detail in a previous study that employed an identical model and found no regional differences in lung wet/dry ratios or wet/hydroxyproline ratios (5).

Hemodynamics, Gas Exchange, and Lung Volumes

As has previously been observed (4–6), turning prone had little effect on hemodynamics or ABGs in normal healthy animals. Because we only studied four animals under control conditions, our type II error is too large for confidence that no positional difference in these variables might exist (e.g., trends toward higher CO, higher Pa_{O_2}, and lower A-aDO_2 were observed). The effect of the prone position on these variables in animals with OA-induced acute lung injury was also similar to previous observations (1, 2).

Heterogeneity of Vr/Qr

Beck and colleagues (12), using MIGET, found that V/Q heterogeneity decreased in normal dogs when they were turned from supine to prone. Our estimate of V/Q heterogeneity (the coefficient of variation of distribution of relative Vr/Qr) also decreased in control animals when they were turned from supine to prone, as was also seen in the OA-injured animals (Table 2). These coefficients should be considered as the lower bound on the true Vr/Qr heterogeneity due to the relatively limited resolution of SPECT. The rightward shift in the frequency distribution of relative Vr/Qr that we observed in prone compared with supine animals under control conditions (Figure 3) and after OA (Figure 4) indicates a reduction in amount of lung affected by shunt and low relative Vr/Qr consistent with previous MIGET data (4, 12).

Spatial Relationship of Vr/Qr (Supine versus Prone)

The reduction in the gravitational Ppl gradient that occurs on turning prone has been directly measured in dogs, rabbits, horses, and pigs (7, 8, 10, 13), and has been inferred from studies of regional lung volume in dogs and sloths (14–16). That a similar change occurs in humans is suggested by measurements of the effects of prone position on regional FRC (17–19) and on the single breath oxygen test (20–22). In addition, Orphanidou and colleagues (23) studied normal human subjects with SPECT and found that the gravitational distribution of Vr was more uniform in prone compared with supine position.

The generally accepted model of regional ventilation described by Milic-Emili and colleagues (18), based on the existence of a gravitational Ppl gradient, together with the fact that lung edema increases the Ppl in the dorsal lung regions of supine animals (10), predicts that this decrease in ventilation resulting from lung injury would primarily occur in dorsal regions as a result of Ptp not exceeding airway opening pressure in this area when supine. The weight of the heart on the dorsal lung is known to contribute to this problem (24–26), as are the effects of the supine position on chest wall shape (25, 26). Our observation that perfusion redistribution away from these areas occurs to only a minor extent in the setting of lung injury (5), predicts that this decreased dorsal Vr would result in shunt and low Vr/Qr.

The effect of posture on Ppl in dependent regions and on the gravitation Ppl gradient (7–10, 26) predicts that, on turning prone, Vr would be more uniform as the Ptp in both dorsal and ventral regions would exceed, or at least would more closely approximate, airway opening pressure. That this change would be associated with reduction in shunt and low V/Q is predicted by the observations that (*1*) regional perfusion in the setting of lung injury is relatively unaffected by a change in posture (5, 12), (*2*) vascular conductance in dorsal lung regions is increased (favoring increased Qr to dorsal lung even when dorsal regions are in the nondependent position) (27), and (*3*) gravity has a very limited effect on Qr

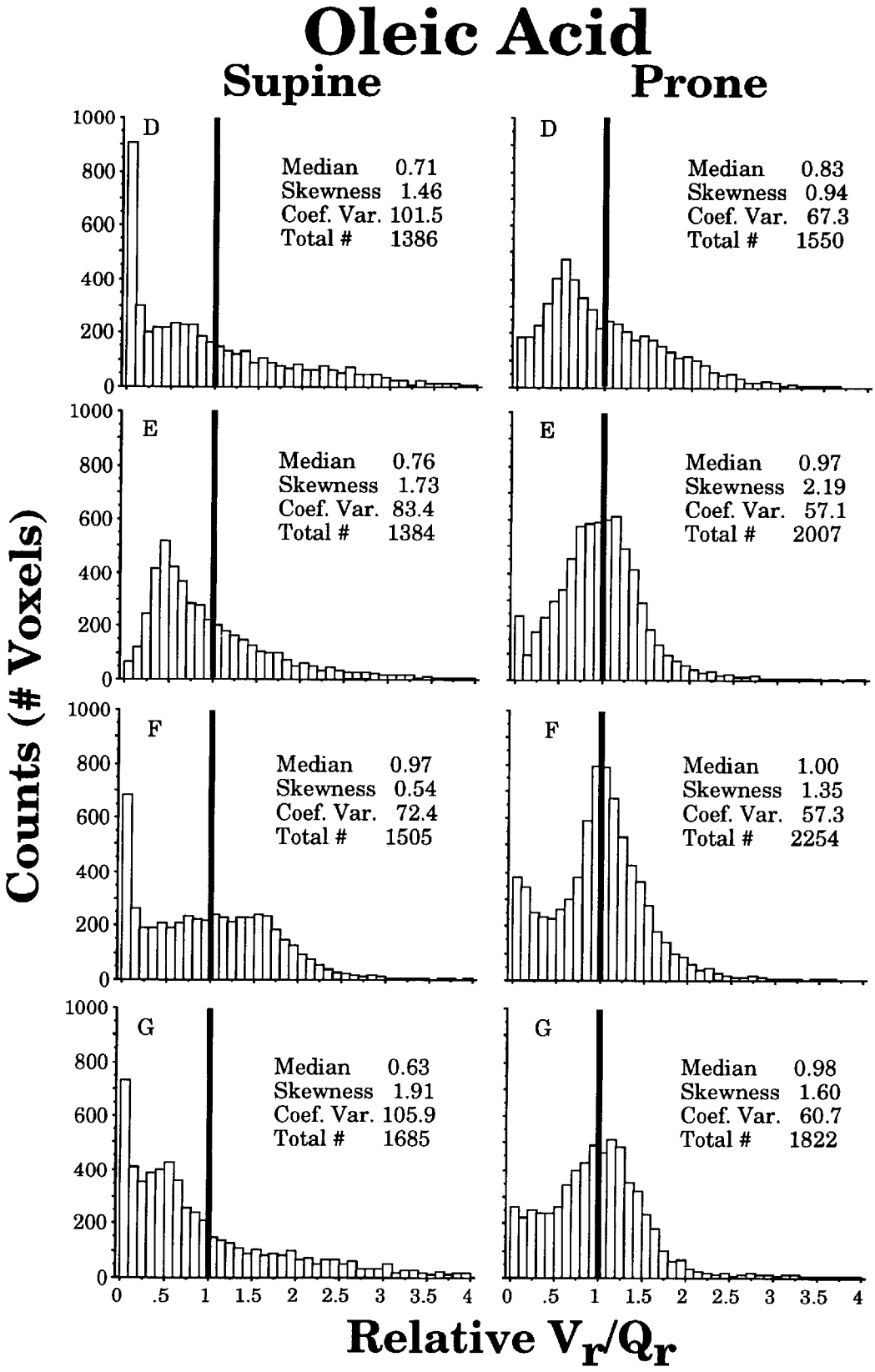

Figure 4. Frequency distribution of relative Vr/Qr for each oleic acid injured animal in the supine and prone condition. Capital letters represent individual animals.

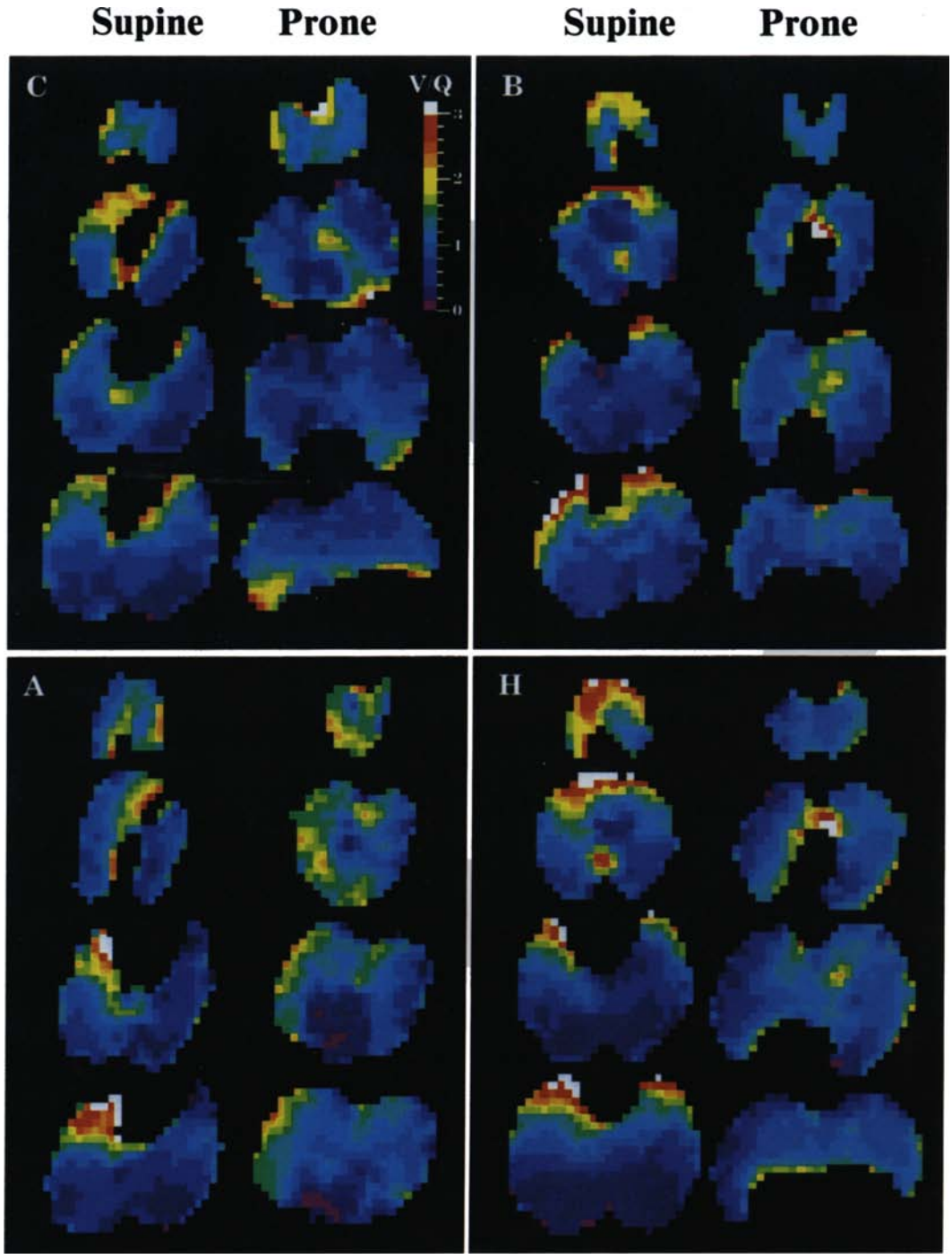

Figure 5. Reconstructed tomographic images of relative Vr/Qr in control animals scanned in supine and prone condition. The four transverse slices are ~ 4 cm apart and are oriented cranial to caudal (*top to bottom*).

distribution in Zone 3 lungs (28). Our data are completely consistent with this explanation.

In this regard, it is of particular interest that the areas of shunt seen in the supine SPECT scans (i.e., Vr/Qr < 0.3) are not randomly distributed in the lung, or even randomly distributed in the dorsal regions. Rather, they seem to develop quite abruptly along the gravitational axis (Figure 6), as would be expected if reduced ventilation were the result of the regional gradient in Ppl, and therefore, the regional gradient in Ptp, not exceeding airway opening pressure. The observation that relative Vr/Qr in the dorsal regions improves as rapidly as the animals are turned prone (e.g., ABGs improve within the first 5 min, SPECT scans change in the first 30 min) is also compatible with this explanation as the change in the relationship between Ptp and airway opening pressure should occur as rapidly as body position is altered.

In summary, interpreting our data along with other studies in the literature indicates that, after OA injury, (*1*) Vr to large areas in the dorsal lung regions decreases or ceases while Qr to this area is relatively maintained, and (2) on turning prone, dorsal lung V improves, ventral lung V is diminished (albeit to a lesser extent than the improvement in dorsal lung V) and Qr is generally unchanged. These findings explain the improvement in oxygenation that occurs on turning prone.

Our findings support the importance of regional Ppls (and re-

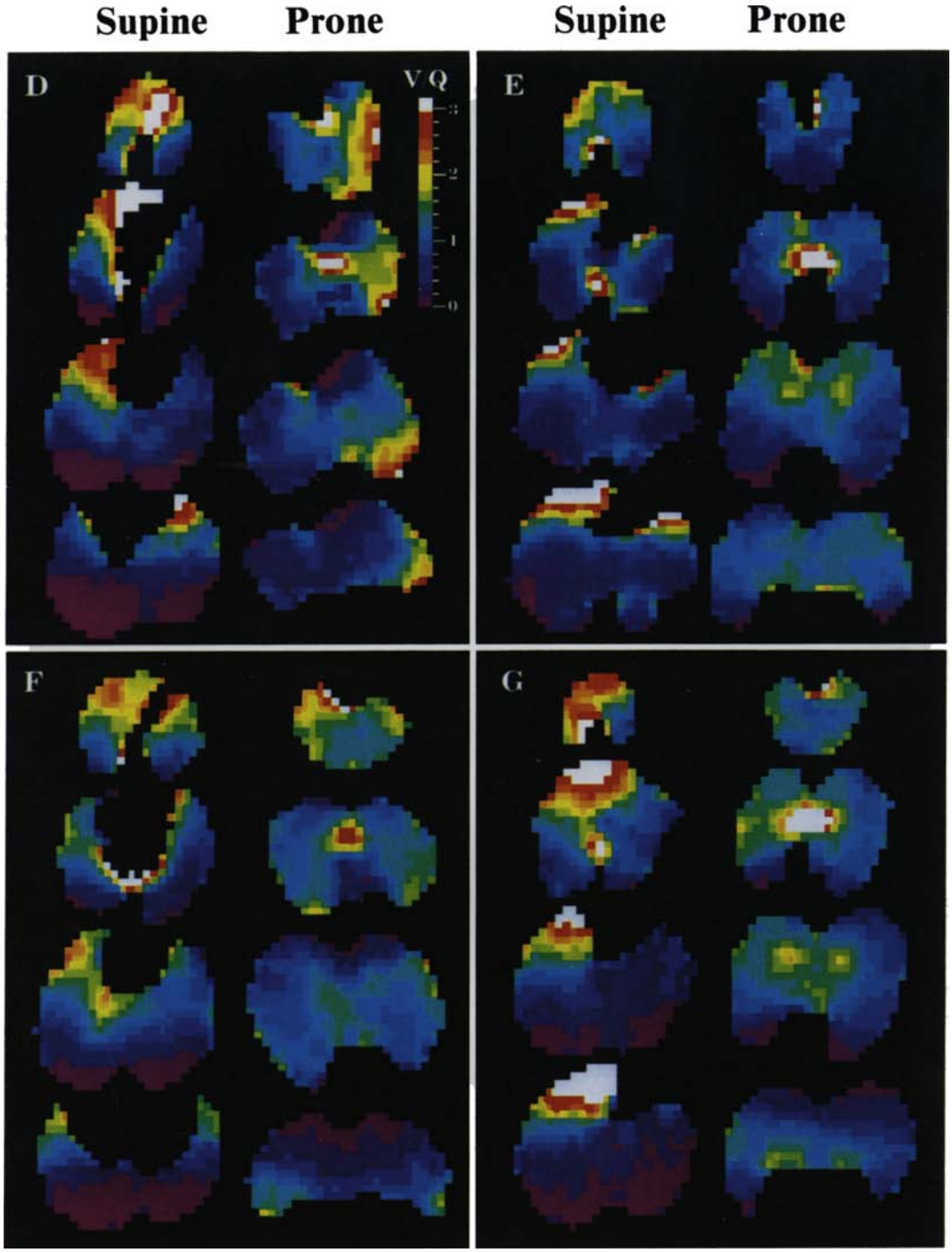

Figure 6. Reconstructed tomographic images of relative Vr/Qr in the supine and prone conditions for all four animals receiving oleic acid.

gional Ptps) in determining Vr and, consequently, the degree of shunt and V/Q heterogeneity seen in the setting of lung injury. Although PEEP can increase airway and alveolar pressure to the point that Ptp exceeds airway opening pressure despite positive Ppl, a more direct approach to the problem (i.e., the positive Ppl) would be to turn prone. Although some technical and practical difficulties may limit the ability to manage some ARDS patients in the prone position, the improvements in physiology that result will frequently allow use of lower levels of PEEP and reduced FI_{O_2}.

References

1. Douglas WW, Rehder K, Beynen RM, Sessler AD, Marsh HM. Improved oxygenation in patients with acute respiratory failure: the prone position. Am Rev Respir Dis 1977;115:559–66.
2. Langer M, Mascheroni D, Marcolin R, Gattinoni L. The prone position in ARDS patients. A clinical study. Chest 1988;94:103–7.
3. Piehl MA, Brown RS. Use of extreme position changes in respiratory failure. Crit Care Med 1976;4:13–4.
4. Albert RK, Leasa D, Sanderson M, Robertson HT, Hlastala MP. The prone position improves arterial oxygenation and reduces shunt in oleic-acid-induced acute lung injury. Am Rev Respir Dis 1987;135:628–33.
5. Wiener CM, Kirk W, Albert RK. Prone position reverses gravitational distribution of perfusion in dog lungs with oleic acid-induced injury. J Appl Physiol 1990;68:1386–92.
6. Glenny RW, Lamm WJE, Albert RK, Robertson HT. Gravity is a minor determinant of pulmonary blood flow distribution. J Appl Physiol 1991;71:620–9.
7. Lai-Fook SJ, Beck KC, Sothorn PA. Pleural liquid pressure measured by

micropipettes in rabbits. J Appl Physiol 1984;56:1633–9.
8. Wiener-Kronish JP, Gropper MA, Lai-Fook SJ. Pleural liquid pressure in dogs measured using a rib capsule. J Appl Physiol 1985;59:597–602.
9. Yang Q-H, Kaplowitz MR, Lai-Fook SJ. Regional variations in lung expansion in rabbits: prone vs. supine positions. J Appl Physiol 1989; 67:1371–6.
10. Mutoh T, Guest RJ, Lamm WJE, Albert RK. Prone position alters the effect of volume overload on regional pleural pressures and improves hypoxemia in pigs *in vivo*. Am Rev Respir Dis 1992;146:300–6.
11. Feldman HA. Families of lines: random effects in linear regression analysis. J Appl Physiol 1988;64:1721–32.
12. Beck KC, Vettermann J, Rehder K. Gas exchange in dogs in the prone and supine positions. J Appl Physiol 1992;72:2292–7.
13. Olson LE, Lai-Fook SJ. Pleural liquid pressure measured with rib capsules in anesthetized ponies. J Appl Physiol 1988;64:102–7.
14. Hoffman EA, Ritman EL. Effect of body orientation on regional lung expansion in dog and sloth. J Appl Physiol 1985;59:481–91.
15. Hoffman EA. Effect of body orientation on regional lung expansion: a computed tomographic approach. J Appl Physiol 1985;59:468–80.
16. Hubmayr RD, Walters BJ, Chevalier PA, Rodarte JR, Olson LE. Topographical distribution of regional lung volume in anesthetized dogs. J Appl Physiol: Respirat Environ Exercise Physiol 1983;54:1048–56.
17. Amis TC, Jones HA, Hughes JMB. Effect of posture on inter-regional distribution of pulmonary ventilation in man. Respir Physiol 1984;56:145–67.
18. Kaneko K, Milic-Emili J, Dolovich MB, Dawson A, Bates DV. Regional distribution of ventilation and perfusion as a function of body position. J Appl Physiol 1966;21:767–77.
19. Amis TC, Jones HA, Hughes JMB. Effect of posture on inter-regional distribution of pulmonary perfusion and V_A/Q in man. Respir Physiol 1984;56:169–82.
20. Clarke SW, Jones JG, Glaister DH. Changes in pulmonary ventilation in different postures. Clin Sci 1969;37:357–69.
21. Cortese DA, Rodarte JR, Rehder K, Hyatt RE. Effect of posture on the single-breath oxygen test in normal subjects. J Appl Physiol 1976; 41:474–9.
22. Lai Y-L, Rodarte JR, Hyatt RE. Effect of body position on lung emptying in recumbent anesthetized dogs. J Appl Physiol: Respirat Environ Exercise Physiol 1979;46:716–20.
23. Orphanidou D, Hughes JMB, Myers MJ, Al-Suhali A-R, Henderson B. Tomography of regional ventilation and perfusion using krypton 81m in normal subjects and asthmatic patients. Thorax 1986;41:542–51.
24. Wiener CM, McKenna WJ, Myers MJ, Lavender JP, Hughes JMB. Left lower lobe ventilation is reduced in patients with cardiomegaly in the supine but not the prone position. Am Rev Respir Dis 1990;141:150–5.
25. Margulies SS, Rodarte JR. Shape of the chest wall in the prone and supine anesthetized dog. J Appl Physiol 1990;68:1970–8.
26. Liu S, Margulies SS, Wilson TA. Deformation of the dog lung in the chest wall. J Appl Physiol 1990;68:1979–87.
27. Beck KC, Rehder K. Differences in regional vascular conductances in isolated dog lungs. J Appl Physiol 1986;61:530–8.
28. Glenny RW, Polissar L, Robertson HT. Relative contribution of gravity to pulmonary perfusion heterogeneity. J Appl Physiol 1991;71:2449–52.